THE JOURNAL OF BIOLOGICAL CHEMISTRY VOL. 287, NO. 43, pp. 35964–35974, October 19, 2012

Afadin Is Required for Maintenance of Dendritic Structure and Excitatory Tone*[S]

Received for publication, March 20, 2012, and in revised form, August 14, 2012 Published, JBC Papers in Press, September 4, 2012, DOI 10.1074/jbc.M112.363358

Deepak P. Srivastava[‡§1], Bryan A. Copits[¶], Zhong Xie[‡], Rafiq Huda[‡], Kelly A. Jones[‡], Srishti Mukherji[§], Michael E. Cahill[‡], Jon-Eric VanLeeuwen[‡], Kevin M. Woolfrey[‡], Igor Rafalovich[‡], Geoffrey T. Swanson[¶], and Peter Penzes[‡‖2]

From the Departments of [‡]Physiology, [¶]Molecular Pharmacology and Biological Chemistry, and [‖]Psychiatry and Behavioral Sciences, Northwestern University Feinberg School of Medicine, Chicago, Illinois 60611 and the [§]Department of Neuroscience and Centre for the Cellular Basis of Behaviour, James Black Centre, Institute of Psychiatry, King's College London, London SE5 9NU, United Kingdom

Background: Active molecular mechanisms that maintain the dendritic field of neurons are unclear.
Results: Afadin maintains dendritic arborization, synapse number, and excitatory transmission and interacts with AMPA-GluA2 receptors.
Conclusion: Afadin is required for the maintenance of dendritic structure and synaptic transmission.
Significance: Elucidating the mechanisms required for the active maintenance of dendritic fields may provide insight into the pathophysiology of neuropsychiatric disorders.

The dendritic field of a neuron, which is determined by both dendritic architecture and synaptic strength, defines the synaptic input of a cell. Once established, a neuron's dendritic field is thought to remain relatively stable throughout a cell's lifetime. Perturbations in a dendritic structure or excitatory tone of a cell and thus its dendritic field are cellular alterations thought to be correlated with a number of psychiatric disorders. Although several proteins are known to regulate the development of dendritic arborization, much less is known about the mechanisms that maintain dendritic morphology and synaptic strength. In this study, we find that afadin, a component of N-cadherin·β-catenin·α-N-catenin adhesion complexes, is required for the maintenance of established dendritic arborization and synapse number. We further demonstrate that afadin directly interacts with AMPA receptors and that loss of this protein reduces the surface expression of GluA1- and GluA2-AMPA receptor subunits. Collectively, these data suggest that afadin is required for the maintenance of dendritic structure and excitatory tone.

The size and shape of dendritic arbors define a neuron's dendritic field (1). Moreover, the number and distribution of neurotransmitter receptors across the dendritic field play a critical role in establishment of synaptic tone, which is a reflection of the synaptic inputs that impinge on a neuron. These parameters are sustained over the lifetime of individual neurons, in the face of changes in local microenvironments (1, 2), and are therefore integral to maintaining neural circuit function (2). Importantly, maintenance of dendritic morphology and excitatory tone are crucial elements underlying neuronal computational capabilities (3, 4).

To date, much work has focused on mechanisms of neurite outgrowth and the initial establishment of dendritic patterning. Early outgrowth is guided by both intrinsic factors, such as transcription factors (5), and extracellular cues, such as neurotrophins (6). Later in development, adhesion proteins help refine dendritic patterning (2) and establish proper synaptic partners (7, 8). Following the establishment of dendritic fields, the dendritic arbor of a neuron remains relatively stable over the life span of the neuron, with only small alterations in arborization occurring in response to physiological stimuli (1, 2).

How is constancy in dendritic fields achieved while neurons are challenged by external and internal flux? One mechanism is the coordinated regulation of dendritic architecture with excitatory synaptic strength. During development, N-cadherin·β-catenin·α-N-catenin adhesion complexes fulfill a key role in these processes (1, 2, 9, 10). Although overexpression of components of the N-cadherin·β-catenin·α-N-catenin adhesion complex can enhance dendritic growth in a transcription-independent manner (9, 10), overexpression of β-catenin itself results in reduced synaptic transmission and surface expression of the AMPA receptor (AMPAR)[3] subunit GluA1 (9). Conversely, removal of postsynaptic β-catenin decreases dendritic

* This work was supported, in whole or in part, by National Institutes of Health (NIH) Ruth L. Kirschstein National Research Service Awards 1F31MH087043 (to J. E. V.), 1F31AG031621 (to M. E. C.), and 1F31MH085362 (to K. A. J.); NIH, NIMH, Grants MH071316 and MH097216 (to P. P.); and NIH, NINDS, Grant NS44322 (to G. T. S.). This work was also supported by grants from the Royal Society UK, American Heart Association (AHA), and National Alliance for Research on Schizophrenia and Depression (NARSAD) (to D. P. S.); an AHA predoctoral fellowship (to K. M. W.); and an Autism Speaks, NARSAD, Brain Research Foundation grant (to P. P.).
[S] This article contains supplemental Figs. 1–3.
[1] To whom correspondence may be addressed: Dept. of Neuroscience and Centre for the Cellular Basis of Behaviour, James Black Centre, Institute of Psychiatry, King's College London, London SE5 9NU, United Kingdom. E-mail: deepak.srivastava@kcl.ac.uk.
[2] To whom correspondence may be addressed: Dept. of Physiology, Northwestern University Feinberg School of Medicine, 303 E. Chicago Ave., Chicago, Illinois 60611. E-mail: p-penzes@northwestern.edu.

[3] The abbreviations used are: AMPAR, AMPA receptor; mEPSC, miniature excitatory postsynaptic current; DIV, day(s) *in vitro*; TDL, total dendritic length; TDN, total dendrite number.

branching but increases miniature excitatory postsynaptic current (mEPSC) amplitudes (9). Although these data demonstrate an inverse relationship between dendritic structure and synaptic function mediated by the N-cadherin·β-catenin·α-N-catenin adhesion complex (9, 10), they nevertheless indicate that dendritic morphology and excitatory tone are regulated in a coordinated manner.

Aiming to further investigate whether dendritic structure and excitatory tone could be coordinated in a similar manner in neurons with established dendritic fields, we hypothesized that additional components of this adhesion complex might have similar functions. The PDZ domain-containing scaffolding protein afadin (also known as AF-6), which directly associates with the N-cadherin·β-catenin·α-N-catenin adhesion complex (11, 12), has recently been shown to be required for the development of excitatory synapses and synaptic transmission in the hippocampus (13, 14). However, whether afadin plays a critical role in the maintenance of mature dendrite arbors and excitatory tone is not known. Here we show that knockdown of afadin in cortical pyramidal neurons with established dendritic fields results in the simplification of the dendritic tree and a reduction in AMPAR-mediated mEPSCs. We further observe a concurrent loss of excitatory synapses and surface expressing GluA1- and GluA2-containing AMPARs. Moreover, we demonstrate that afadin directly interacts with the GluA2 subunit, providing a molecular substrate for the regulation of neuronal excitatory tone. Together, these data suggest that afadin is required for the maintenance of dendritic fields through the coordinated regulation of dendrite morphology, synapse structure, and function.

EXPERIMENTAL PROCEDURES

Reagents—The following antibodies were purchased. GFP mouse monoclonal (MAB3580), N-terminal GluA2 mouse monoclonal (MAB397), and VGlut1 (vesicular glutamate transporter 1; MAB5502) mouse monoclonal antibodies were from Millipore, and other antibodies were as follows: GFP chicken polyclonal (ab13972; Abcam), PSD-95 mouse monoclonal (73-028; NeuroMab), Myc mouse monoclonal (9E10; Developmental Studies Hybridoma Bank, Iowa City, IA), and L/S-afadin (AF-6; A0224) (Sigma). Rabbit polyclonal antibodies against GFP, N-terminal GluA1, C-terminal GluA1, and N-terminal GluA2/3 were a kind gift from Dr. Richard Huganir (Johns Hopkins University). Phalloidin (*Amanita phalloides* toxin) was from Invitrogen. Plasmids used in this study were GFP-PSD-95, GFP-GluA1 (flop), GFP-GluA2 (flop) and myc-L-afadin (12, 15).

Neuronal Culture and Transfections—Medium and high density cortical neuron cultures were prepared from Sprague-Dawley rat E18 embryos as described previously (16). Briefly, neurons were plated onto coverslips coated with poly-D-lysine (0.2 mg/ml; Sigma), in feeding medium (Neurobasal medium supplemented with B27 (Invitrogen) and 0.5 mM glutamine). 200 μM DL-aminophosphonovalerate (Ascent Scientific) was added to the medium 4 days later. Cortical neurons were transfected at day *in vitro* (DIV) 23 using Lipofectamine 2000 following the manufacturer's recommendations (16). Transfections were allowed to carry on for 5 days (unless stated otherwise). Neurons were then fixed in 4% formaldehyde, 4% sucrose PBS for 10 min. Coverslips were then processed for immunostaining. Only neurons that exhibited a pyramidal asymmetric morphology, with a single long, highly branching protrusion, likely to be the apical dendrite, and many shorter dendrites radiating from the soma, likely to be the basal dendrites, were selected for further analysis (16, 17). Any signs of poor neuronal health, such as "blebbing" or other irregularities in the dendritic membrane, or an abnormally shaped soma were criteria for exclusion of the cell from quantification.

Cell Cultures—HEK293 cells were cultured in DMEM with 10% FCS and penicillin/streptomycin. Cells were plated onto 6-well plates and grown until 50% confluence, when they were transfected using Lipofectamine 2000. Between 2 and 5 μg of DNA was used with 3 μl of Lipofectamine 2000/well, transfections proceeded for 48 h, and cells were then harvested for biochemistry.

RNA Interference—Several gene-specific inserts were designed using the BLOCK-iT software (Invitrogen) to encode 21-nucleotide sequences derived from the rat afadin sequence, separated by spacer loops of 9 nucleotides, followed by the reverse complement sequence of the target sequence, and subcloned into the pGsuper vector (18), which expresses shRNA and enhanced GFP simultaneously, allowing identification of transfected cells and outlining neuronal morphology. The sequence corresponding to nucleotides 4918–4929 of rat afadin cDNA was targeted, ensuring that both isoforms (L- and S-afadin) would be targeted (target sequence, 5′-gcaacagcaaatgcacattgt-3′). A control shRNA (mut-shRNA) was generated by inserting three point mutations into the recognition sequence of the shRNA (afadin-shRNA sequence, 5′-gcaacagcaaatgcacattgt-3′; mut-shRNA sequence, 5′-gcaacaTcaaatgcGcattAt-3′). An RNAi-insensitive afadin construct was generated by inserting three non-coding point mutations into the RNAi recognition site in a myc-L-afadin plasmid ("rescue"; mutated target sequence, 5′-gcaGcagcaaatgcaTatCgt-3′).

Immunocytohistochemistry—Transfected neurons were fixed as above. For the staining of endogenous proteins, medium density DIV 25 neurons were first washed in PBS and then fixed in either 4% formaldehyde, 4% sucrose PBS for 10 min, followed by incubation in methanol prechilled to −20 °C for 10 min, or in methanol only, prechilled to −20 °C for 20 min. Fixed neurons were then permeabilized and blocked simultaneously before incubation in primary antibodies as described previously (16). In the green/purple color scheme, colocalization is indicated by white overlap. All images were acquired in the linear range.

AMPA Receptor Surface Labeling and Staining—Transfected neurons (DIV 28) were used to label surface GluA1 and GluA2. Live cells were incubated with either n-GluA1 or n-GluA2 antibodies (1:100 dilution) at 4 °C for 30 min in artificial cerebrospinal fluid, as described previously (19, 20). Neurons were then fixed for 5 min in 4% formaldehyde, 4% sucrose in PBS. Cells were then processed for immunocytohistochemistry as described above.

Dendrite Visualization and Quantitative Morphometric Analysis—To quantify dendritic morphology, pyramidal neurons expressing enhanced GFP were imaged using a ×10 objec-

tive (numerical aperture = 0.17), and micrographs were acquired using a Zeiss AxioCam MRm CCD camera. Following acquisition, dendrites were traced and binarized in ImageJ (National Institutes of Health, Bethesda, MD). Only cells exhibiting intact healthy secondary and tertiary apical and basal dendrites were imaged and used for quantification. The axon was identified by its distinct morphology and was eliminated from quantification. Dendritic length and branch number were analyzed using the NeuronJ plugin for ImageJ. Sholl analysis was performed using the Sholl analysis plugin for ImageJ (available on the World Wide Web) to measure the number of dendritic processes that intersected with concentric circles spaced 25 μm apart starting at the center of the soma. For each parameter, 11 cells from four experiments were measured, and images were acquired and quantified by an experimenter blind to condition.

Quantitative Analysis of Spine Morphologies and Immunofluorescence—Images of dendritic spines and surface-GluA2 immunostaining were acquired from the same cells used for dendrite analysis. Cells used for surface GluA1 staining were processed separately. Confocal images of double-stained neurons were obtained as described previously (16). Briefly, images were acquired with a Zeiss LSM5 Pascal confocal microscope using a ×63 oil immersion objective (Zeiss; numerical aperture = 1.4) as a *z*-series. The acquisition parameters were kept the same for all conditions. Two-dimensional maximum projection reconstructions of images were generated, and morphometric analysis (spine number, area, and breadth) was done using MetaMorph software (Universal Imaging) (16). Cultures that were directly compared were stained simultaneously and imaged with the same acquisition parameters. For each condition, 11–12 neurons each from at least three separate experiments were used. For overall dendritic spine linear density measurements (spines/10 μm), at least two dendrites (secondary or tertiary branches), totaling 100 μm, from each neuron were analyzed. For dendritic spine linear density as a function of dendritic branch order, between 20 and 50 μm of dendritic length along at least 1–2 dendritic branches of each order (primary, secondary, or tertiary) were analyzed per neuron. Experiments were done blind to conditions and on sister cultures. To examine the morphologies of dendritic spines, individual spines on dendrites were manually traced, and spine dimensions were measured by MetaMorph.

To analyze the surface expression of GluA1 and GluA2, transfected neurons were visualized with antibodies against the appropriate protein, and immunofluorescence was quantified using MetaMorph (16). Images were acquired as described above. The background corresponding to areas without cells was subtracted to generate a "background-subtracted" image. Images were then thresholded equally to include clusters with intensity at least 2-fold above the adjacent dendrite. Dendritic spines were designated as "regions," and the linear density (number/10 μm of dendrite length), area, and total gray value (total immunofluorescence intensity) of each AMPA receptor cluster were measured automatically (16). Cultures that were directly compared were stained simultaneously and imaged with the same acquisition parameters (16). Experiments were carried out blind to condition and on sister cultures. All statistical analysis was performed as described below.

Coimmunoprecipitation—For co-immunoprecipitation assays in HEK293 cells, transfected cells were harvested in radioimmune precipitation assay lysis buffer (150 mM NaCl, 10 mM Tris-HCl, pH 7.2, 5 mM EDTA, 0.1% SDS, 1% Triton X-100, 1% deoxycholate plus protease inhibitors). Lysates were then sonicated and cleared by centrifugation at 14,000 × *g* for 10 min. Lysates were precleared with 30 μl of protein-Sepharose A for 60 min at 4 °C. Resin was pelleted, and the supernatants were then incubated with 3–5 μl of the appropriate antibody for 4 h. Finally, 60 μl of protein-Sepharose A was then added to the samples and incubated for 2 h at 4 °C, after which samples were washed three times with radioimmune precipitation assay buffer.

Coimmunoprecipitations of mouse frontal cortex were carried essentially as described above. Mouse frontal cortex was dissected from 8-week-old C57/B6 mice. All animal procedures were carried out according to Northwestern University and animal care and use committee-approved protocols. Tissue was then lysed in radioimmune precipitation assay buffer and sonicated, and cell debris was removed by centrifugation. This was followed by a preclearing stage, where lysates were incubated with 30 μl of protein-Sepharose A for 60 min at 4 °C. Resin was pelleted, and the supernatants were then incubated with 3–5 μl of the appropriate antibody for 4 h. Finally, 60 μl of protein-Sepharose A was added to the samples and incubated for 2 h at 4 °C, after which samples were washed three times with radioimmune precipitation assay buffer. All samples were boiled for 5 min at 95 °C after the addition of Laemmli buffer and stored at −80 °C until they were resolved by SDS-PAGE and Western blotting. Quantification of bands was performed as described previously (19).

Electrophysiology—Cultured cortical neurons were recorded in whole-cell configuration 5–6 days post-transfection. The extracellular solution contained 140 mM NaCl, 10 mM glucose, 10 mM HEPES, 3 mM KCl, 2 mM $CaCl_2$, 1 mM $MgCl_2$ (pH 7.3). Patch pipettes were pulled from borosilicate glass and fire-polished to a resistance of 3–5 megaohms. The intracellular patch-pipette solution contained 95 mM CsF, 25 mM CsCl, 10 mM HEPES, 10 mM EGTA, 2 mM NaCl, 2 mM Mg-ATP, 10 mM QX-314, 5 mM tetraethylammonium chloride, 5 mM 4-aminopyridine (pH 7.2). Neurons were voltage-clamped at −70 mV, and currents were recorded using pClamp9 software (Molecular Devices, Sunnyvale, CA) with an Axopatch 200B amplifier (Molecular Devices). mEPSCs were isolated by bath application of 10 μM bicucculine, 50 μM picrotoxin, 50 μM DL-aminophosphonovalerate, and 1 μM tetrodotoxin. Verification that mEPSCs were mediated by AMPARs was achieved by adding 50 μM CNQX at the end of recordings. Recordings were filtered at 5 kHz and digitized at 20 kHz. The data were low pass-filtered using a 1 kHz cut-off and analyzed off-line with Mini-Analysis software (Synaptosoft, Fort Lee, NJ).

Statistical Analysis—For quantitative immunofluorescence experiments, co-immunoprecipitations, and dendrite length or number measurements, differences between condition means were identified by Student's unpaired *t* tests or analyses of variance performed in SPSS. Tukey-b post hoc analysis was used for multiple comparisons. *Error bars* represent S.E. For dendrite analysis, the main effects and simple effects were probed by Student's unpaired *t* tests or by one- or two-way analyses of

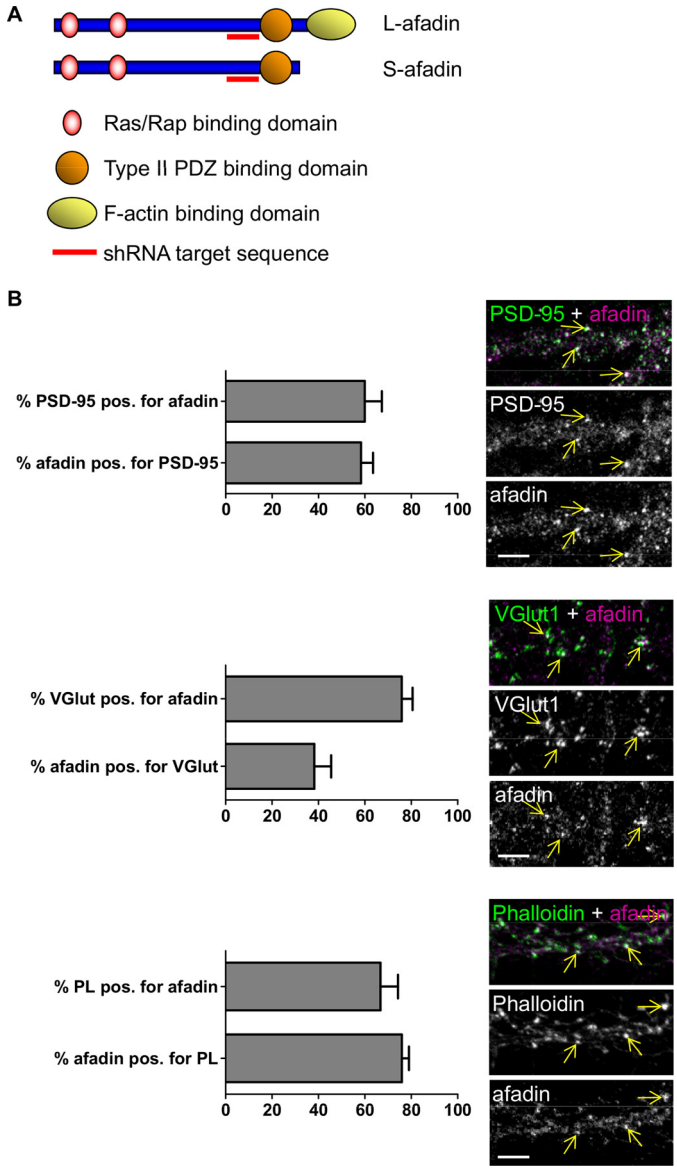

FIGURE 1. **Localization of afadin at excitatory synapses.** *A*, structure of afadin. Both isoforms of afadin contain two Ras/Rap binding domains and a type II PDZ domain. Only L-afadin contains an F-actin binding domain. *B*, localization of afadin in DIV 25 cortical neurons. Shown is double immunofluorescence with antibodies against synaptic proteins PSD-95 and VGlut1 or staining with phalloidin to label F-actin and L/S-afadin. Shown is quantification of the percentage of colocalization of afadin and synaptic proteins PSD-95 and VGlut1 or F-actin. *Yellow arrows* indicate colocalization. $n = 8–11$ cells from three experiments. *Scale bar*, 5 μm. *Error bars*, S.E.

variance with Bonferroni correction for multiple comparisons when appropriate. For mEPSC amplitude and frequency analysis, differences between conditions were determined by Student's unpaired *t* tests.

RESULTS

Afadin Is Found at Excitatory Synapses—Afadin is a multidomain protein containing a Rap/Ras-binding domain and a type II PDZ domain. Two isoforms exist within the brain, long and short afadin (L-afadin and S-afadin), with the longer form containing an F-actin binding motif (Fig. 1*A*). Previous studies have demonstrated that afadin is a key component of epithelial junctions (11), and more recently it has been shown that afadin is present at synapses, where it interacts with N-cadherin·β-catenin·α-N-catenin complexes (12). Moreover, afadin signaling has been shown to be required for both Rap- and Rac-dependent remodeling of dendritic spine morphology following activity-dependent stimuli, adhesion signaling, or rapid estrogen signaling (12, 15, 19). Consistent with this role in the modulation of dendritic spines, electron microscopy of endogenous afadin has localized this protein to synapses (21, 22). To determine whether afadin is present at excitatory synapses in cortical neurons, we examined the location of endogenous afadin, using an antibody that recognizes both L- and S-afadin, in cultured cortical neurons, grown for 25 DIV. We found that afadin partially co-localized with PSD-95 (~60% of PSD-95 puncta co-localized with afadin, whereas ~65% of afadin was positive for overlap with PSD-95; $n = 8–11$ cells from three experiments; Fig. 1*B*) and the excitatory presynaptic marker VGlut1 (vesicular glutamate transporter 1; ~75% of VGlut1 overlapped with afadin; ~56% of afadin co-localized with VGlut1; Fig. 1*B*). Using the *A. phalloides* toxin to stain filamentous actin, we found that afadin puncta co-localized with F-actin (~70%; Fig. 1*B*), suggesting that afadin is indeed well placed to influence actin remodeling, an essential component required for the maintenance of dendrite and synapse structure. Together, these data indicate that a significant portion of afadin (>60%) co-localizes with excitatory synapse markers and F-actin, placing it at an ideal location to regulate dendrite and synapse structure as well as excitatory function.

Characterization of Afadin-shRNA—To investigate whether afadin is required for the maintenance of dendritic morphology and excitatory tone, we employed a short hairpin RNA interference (shRNA) strategy to knock down the expression of endogenous afadin in neurons. We generated an shRNA construct (afadin-shRNA) specifically targeting both isoforms of afadin (Fig. 1A) and a mutant shRNA construct (mut-shRNA); this construct consisted of the afadin-shRNA sequence but with three point mutations inserted into the target sequence such that it would not recognize afadin. All of the shRNA constructs were cloned into the pGSuper plasmid, which coexpresses enhanced GFP and the shRNA. We also employed a rescue construct that expresses a shRNA-insensitive form of afadin (myc-L-afadin-Res, or rescue). We first tested the efficiency and specificity of afadin-shRNA and the mut-shRNA in HEK293 cells (supplemental Fig. 1*A*). Afadin-shRNA blocked ectopic expression of myc-L-afadin, whereas both the mut-shRNA and the empty vector (pGSuper) had no effect on exogenous afadin expression. Importantly, myc-L-afadin-Res expression persisted in the presence of afadin-shRNA expression. When expressed for 3 days in DIV 23 cortical neurons (*i.e.* DIV 26), afadin-shRNA reduced endogenous levels of afadin by $31.5 \pm 7.1\%$ ($p < 0.05$, $n = 12$) compared with control levels; following 5 days of expression (DIV 28), afadin levels were reduced by $74.1 \pm 3.7\%$ ($p < 0.05$, $n = 12$; supplemental Fig. 1, *B* and *C*). Neither pGSuper nor mut-shRNA significantly altered endogenous afadin expression in cortical neurons after 3 or 5 days of expression ($n = 12$; supplemental Fig. 1, *B* and *C*). The afadin rescue construct (rescue) was also confirmed in cortical neurons even in the presence of afadin-shRNA expression for 5 days (supplemental Fig. 1*B*). Subsequent experiments

were performed following 5 days of afadin-shRNA expression to ensure maximal knockdown of afadin.

Afadin Controls Maintenance of Dendrite Arborization—Because afadin is part of the N-cadherin·β-catenin·α-N-catenin complex (12), a pathway that coordinates dendritic patterning and excitatory tone of a neuron in an inverse manner during development (9), we first questioned whether afadin is required for the maintenance of dendritic arborization of cortical neurons with established dendritic fields. Afadin knockdown for 5 days resulted in a significant reduction (~40%) in total dendritic length (TDL), whereas expression of the mut-shRNA had no effect on TDL compared with pGSuper. This effect was rescued by coexpression of the afadin rescue construct with afadin-shRNA (TDL: pGSuper, 567.7 ± 46.8 μm; mut-shRNA, 552.1 ± 32.7 μm; afadin-shRNA, 274.9 ± 35.6 μm; afadin-shRNA + rescue, 478 ± 36.6 μm; $n = 11$; $p < 0.001$; Fig. 2, *A* and *B*). Furthermore, knockdown of afadin caused a ~35% loss in the total dendrite number (TDN) compared with pGSuper and mut-shRNA but was rescued by the expression of the shRNA-insensitive afadin construct (TDN: pGSuper, 15.5 ± 1.2; mut-shRNA, 14.9 ± 1.1; afadin-shRNA, 10 ± 0.7; $n = 11$; afadin-shRNA + rescue, 13.8 ± 0.8; $p < 0.001$; Fig. 2, *A* and *B*). Upon further examination, we found that knockdown of afadin resulted in a reduction of secondary and tertiary dendrite length; this effect was rescued by myc-L-afadin-Res, (average primary dendrite length: pGSuper, 56.4 ± 7.3 μm; mut-shRNA, 63.5 ± 7.1 μm; afadin-shRNA, 52.7 ± 6.8 μm; afadin-shRNA + rescue, 63.5 ± 7.1 μm; average secondary dendrite length: pGSuper, 196.6 ± 25.9 μm; mut-shRNA, 198.0 ± 18.2 μm; afadin-shRNA, 125.2 ± 13.6 μm; afadin-shRNA + rescue, 191.6 ± 16.4 μm; average tertiary dendrite length: pGSuper, 314.7 ± 23.0 μm; mut-shRNA, 290.62 ± 24.7 μm; afadin-shRNA, 97.0 ± 23.9 μm; afadin-shRNA + rescue, 267.4 ± 18.8 μm; $n = 11$; $p < 0.001$; Fig. 2*C*). In addition, we observed a loss of distal dendrite branches in neurons expressing afadin-shRNA (primary dendrite: pGSuper, 1.2 ± 0.1; mut-shRNA, 1.1 ± 0.1; afadin-shRNA, 1.1 ± 0.136.8; afadin-shRNA + rescue, 1.2 ± 0.2; secondary dendrite: pGSuper, 5.7 ± 0.9; mut-shRNA, 5.8 ± 0.7; afadin-shRNA, 5.6 ± 0.5; afadin-shRNA + rescue, 6.2 ± 1.0; tertiary dendrite: pGSuper, 8.6 ± 0.8; mut-shRNA, 7.9 ± 0.8; afadin-shRNA, 3.2 ± 0.6; afadin-shRNA + rescue, 8.9 ± 0.9; $n = 11$; $p < 0.001$; Fig. 2*C*). We further performed Sholl analysis on all conditions. Consistent with our analysis of TDL and TDN, afadin knockdown reduced dendritic intersections 225–375 μm from the soma; expression of the afadin rescue construct was sufficient to rescue this reduction in dendritic complexity (Fig. 2*D*). Collectively, these data suggest that afadin is required for the maintenance of distal, secondary, and tertiary dendrite length and number.

Loss of Afadin Reduces AMPAR-mediated Transmission—Previously, it has been shown that overexpressing β-catenin in developing hippocampal neurons results in a decrease in surface expression of GluA1-containing AMPAR and reduced mEPSC amplitudes (9), indicating that components of N-cadherin adhesion complexes can regulate excitatory function. Consistent with these data, a recent study demonstrated a reduction in field excitatory postsynaptic potentials at the CA1-CA3 synapse taken from mice lacking afadin from birth (13). This reduction was seemingly driven by postsynaptic mechanisms because both release probability and presynaptic connectivity were unaltered (13), suggesting that afadin may play a role in controlling the formation of excitatory synapses via a postsynaptic mechanism during development. However, it is not known whether loss of afadin would alter AMPAR-mediated transmission and, further, if this protein is required for basal AMPAR-transmission in neurons with a stable dendritic field. To investigate this question, we recorded AMPAR-mediated mEPSCs in cortical neurons with established dendritic fields, in the presence or absence of afadin-shRNA, to understand the functional implications of afadin loss. Cells expressing mut-afadin did not display altered AMPAR transmission compared with untransfected cells (Fig. 2, *E* and *F*). Surprisingly, loss of afadin led to a reduction in mEPSC frequency (~46%) compared with cells expressing the mut-shRNA (mEPSC frequency: unTFXed, 17.8 ± 2.7 Hz; mut-shRNA, 18.9 ± 3.52 Hz; afadin-shRNA, 8.76 ± 1.4 Hz; $n = 16$; $p < 0.001$; Fig. 2, *E* and *F*). Interestingly, we did not observe any alterations in AMPAR-mediated mEPSC amplitude between conditions (mEPSC amplitude: unTFXed, 26.7 ± 1.6 peak amplitude (pA); mut-shRNA, 23.56 ± 1.986 pA; afadin-shRNA, 20.92 ± 1.58 pA; $n = 16$; Fig. 2, *D* and *E*). These findings imply that loss of afadin in postsynaptic cells results in impaired functional excitatory transmission. This could be due to the loss of functional synapses or a dampening of presynaptic release probability at existing synapses. Nevertheless, the absence of change in mEPSC amplitude upon afadin loss is consistent with similar receptor content or conductivity at existing synapses. Moreover, these data suggest that there was no compensatory change in synaptic function at the spared synapses to balance the loss of functional input.

Afadin Is Required for the Maintenance of Synapse Structure—The decrease in mEPSC frequency with afadin knockdown suggested the possibility that afadin knockdown induces a decrease in synapse numbers. To address this possibility, we examined dendritic spines in neurons previously assessed for dendritic arborization. Afadin knockdown resulted in a significant reduction in the linear density of dendritic spines (~40%) compared with pGSuper or mut-shRNA conditions but was rescued in the presence of the shRNA-insensitive afadin construct (spines/10 μm: pGSuper, 6.36 ± 0.2; mut-shRNA, 6.68 ± 0.2; afadin-shRNA, 3.89 ± 0.3; afadin-shRNA + rescue, 6.17 ± 0.2; $n = 11$; $p < 0.001$; Fig. 3, *A* and *B*). A detailed analysis of the linear density of dendritic spines as a function of dendrite branch order (primary, secondary, or tertiary) revealed that in addition to a loss of distal dendrites, afadin loss induced the loss of dendritic spines in secondary and tertiary dendrites (primary dendrite: pGSuper, 4.8 ± 0.7; mut-shRNA, 4.3 ± 0.2; afadin-shRNA, 4.5 ± 0.4; afadin-shRNA + rescue, 4.1 ± 0.6; secondary dendrite: pGSuper, 6.3 ± 0.3; mut-shRNA, 6.0 ± 0.2, afadin-shRNA, 5.1 ± 0.2; afadin-shRNA + rescue, 5.9 ± 0.2; tertiary dendrite: pGSuper, 6.4 ± 0.4; mut-shRNA, 6.0 ± 0.4, afadin-shRNA, 3.5 ± 0.1; afadin-shRNA + rescue, 6.4 ± 0.4; $n = 11$; $p < 0.05$ or 0.001; Fig. 3*C*). A more in depth analysis of dendritic spine morphology further revealed that afadin-shRNA-expressing cells had spines with significantly reduced length and breadth compared with pGSuper or mut-shRNA conditions,

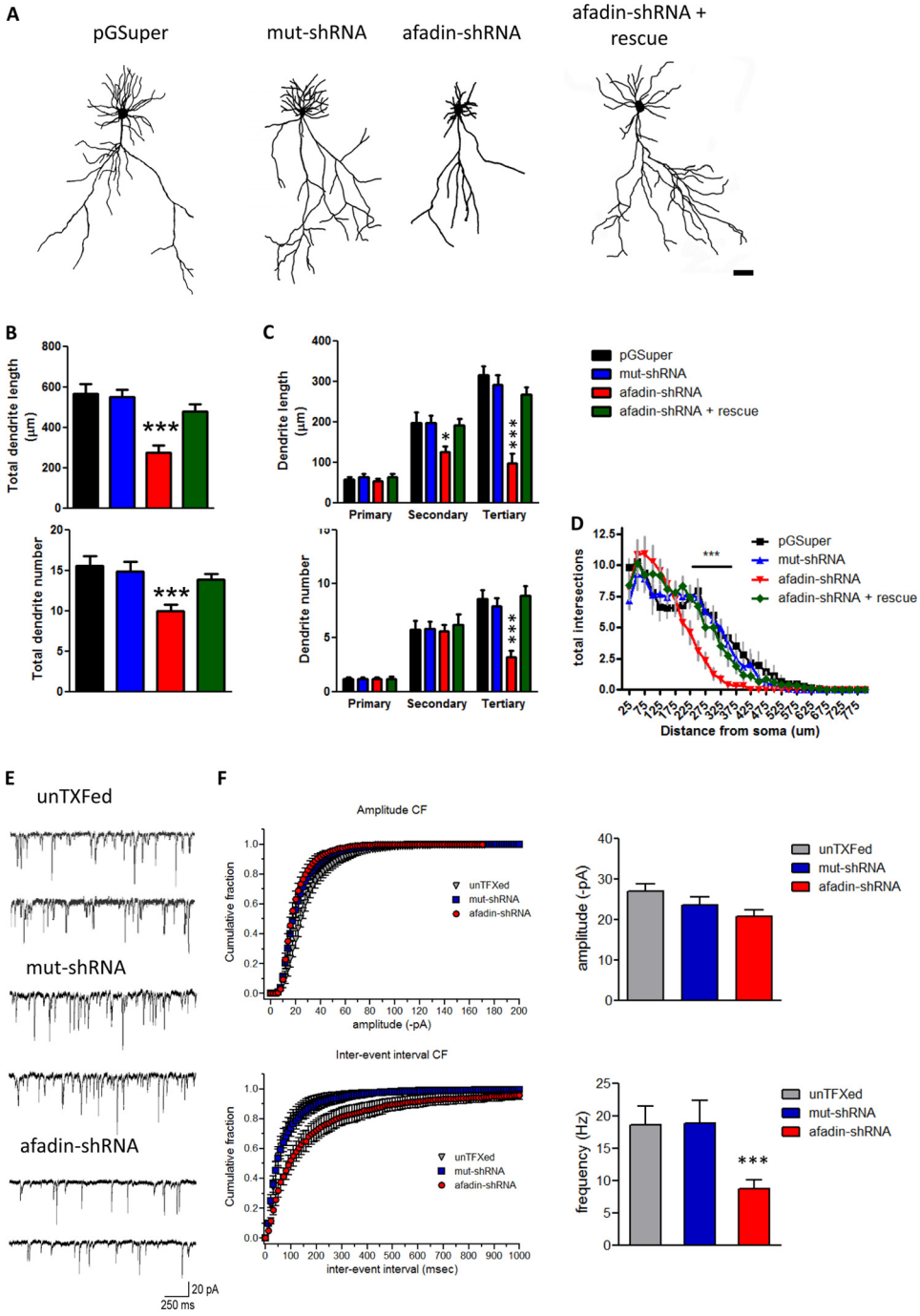

FIGURE 2. **Afadin is required for the maintenance of dendritic architecture and excitatory inputs.** *A*, representative binary images of cortical neurons (DIV 28) expressing pGSuper, control-shRNA, afadin-shRNA, or afadin-shRNA + rescue. *B*, quantification of TDL and TDN of cells in *A* ($n = 11$; ***, $p < 0.001$). *C*, quantification of primary, secondary, and tertiary dendritic length and branch number in cells expressing pGSuper, mut-shRNA, afadin-shRNA, or afadin-shRNA + rescue ($n = 11$; *, $p < 0.05$; ***, $p < 0.001$). *D*, Sholl analysis of dendritic complexity of neurons in *A*. Expression of afadin-shRNA reduces dendritic complexity compared with control conditions, but co-expression of rescue restores dendritic complexity to control levels. *E*, representative AMPAR-mediated mEPSC traces of cells expressing control-shRNA or afadin-shRNA. *F*, quantification of mEPSC amplitude and frequency ($n = 16$ or 15, respectively; ***, $p < 0.001$). *Scale bar*, 50 μm. *Error bars*, S.E.

suggesting a particular deficit in larger spines (supplemental Fig. 2*A*). Indeed, histograms of spine areas demonstrated that expression of afadin-shRNA resulted in a prevalence of spines with a smaller area (supplemental Fig. 2*B*). Furthermore, we assessed the number of spines as a percentage of total spines with distinct spine areas (supplemental Fig. 2*C*). Both pGSuper and mut-shRNA conditions had similar percentages of spines within the defined spine areas. On the other hand, afadin-shRNA-expressing cells had an increase in the number of spines with smaller areas and had no spines with areas larger than 1.2 μm^2 ($n = 11$; supplemental Fig. 2*C*), demonstrating that neurons expressing afadin-shRNA had fewer spines with larger areas and more spines with smaller areas. Collectivity, these data suggest that afadin is required for the maintenance of dendritic spines with large areas in neurons with established dendritic fields.

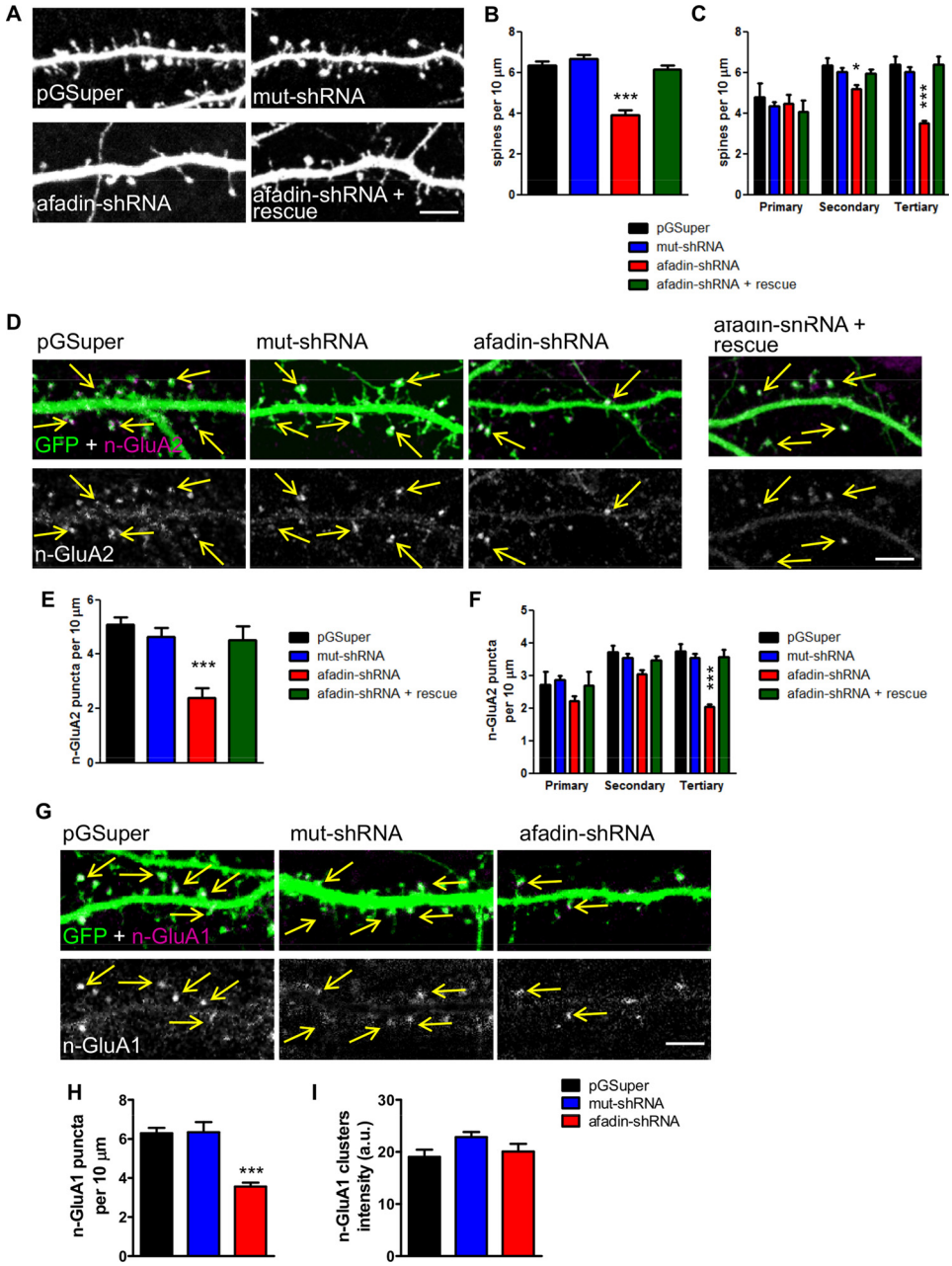

FIGURE 3. **Coordinated regulation of synaptic structure and function by afadin.** *A*, representative high magnification images of neurons expressing pGSuper, mut-shRNA, afadin-shRNA, or afadin-shRNA + rescue. *B* and *C*, quantification of dendritic spines in *A*, either overall (*B*) or as a function of dendritic branch order (*C*) ($n = 11$; *, $p < 0.05$; ***, $p < 0.001$). *D*, example high magnification images of surface GluA2 (n-GluA2) and overlay with GFP, in cells expressing pGSuper, control-shRNA, afadin-shRNA, or afadin-shRNA + rescue. *E* and *F*, quantification of surface-GluA2 puncta number, either overall (*E*) or as a function of dendritic branch order (*F*) in *D* ($n = 11$; *, $p < 0.05$; ***, $p < 0.001$). *G*, example high magnification images of surface GluA1 (n-GluA1) and overlay with GFP in cells expressing pGSuper, control-shRNA, or afadin-shRNA. *H* and *I*, quantification of surface-GluA1 puncta number (*H*) and cluster intensity (*I*) in *G* ($n = 12$, $p < 0.001$). *Scale bars*, 5 μm. *Error bars*, S.E.

Surface Expression of AMPARs Requires Afadin Expression—Because we had observed a reduction in the frequency of AMPAR-mediated transmission, consistent with a loss of synapse number, we next sought to understand whether afadin was required for the synaptic expression of AMPARs. Interestingly, we have previously demonstrated that acute interference with N-cadherin function in mature cortical neurons results in the loss of AMPARs from synapses (12). Because afadin directly interacts with N-cadherin signaling complexes, these data suggest that afadin may indeed be able to regulate AMPAR synaptic expression. We first assessed the surface expression of endogenous GluA2 protein in the population of neurons examined previously for dendritic and synaptic morphology. Afadin knockdown reduced the number of surface-GluA2 puncta (~45%) when compared with pGSuper, mut-shRNA, or rescue conditions (n-GluA2/10 μm: pGSuper, 5.07 ± 0.3; mut-shRNA, 4.63 ± 0.4; afadin-shRNA, 2.39 ± 0.3; afadin-shRNA + rescue, 4.5 ± 0.5; $n = 11$; $p < 0.001$; Fig. 3, *D* and *E*). When we examined surface GluA2 puncta as a function of dendrite branch order, we found that there was a significant reduction of synaptic GluA2 on tertiary dendrites in afadin-shRNA cells compared with control conditions (n-GluA2/10μm: primary

dendrite: pGSuper, 2.7 ± 0.4; mut-shRNA, 2.8 ± 0.1; afadin-shRNA, 2.2 ± 0.2; afadin-shRNA + rescue, 2.7 ± 0.4; secondary dendrite: pGSuper, 3.7 ± 0.2; mut-shRNA, 3.5 ± 0.1, afadin-shRNA, 3.0 ± 0.1; afadin-shRNA + rescue, 3.5 ± 0.1; tertiary dendrite: pGSuper, 3.7 ± 0.2; mut-shRNA, 3.5 ± 0.1; afadin-shRNA, 2.0 ± 0.07; afadin-shRNA + rescue, 3.6 ± 0.2; $n = 11$; $p < 0.001$; Fig. 3*F*). We next examined the number of surface GluA1 puncta in a different set of cells; afadin-shRNA-expressing cells displayed a significantly reduced number of surface-GluA1 puncta compared with pGSuper- or mut-shRNA-expressing cells (n-GluA1/10 μm: pGSuper, 6.3 ± 0.3; mut-shRNA, 6.4 ± 0.5; afadin-shRNA, 3.5 ± 0.2; $n = 12$; $p < 0.001$; Fig. 3, *G* and *H*). Surprisingly, we did not observe any change in surface GluA2 or GluA1 puncta intensity (n-GluA2 cluster intensity: pGSuper, 10.4 ± 0.6 arbitrary units; mut-shRNA, 10.9 ± 0.6 arbitrary units; afadin-shRNA, 9.6 ± 0.4 arbitrary units; $n = 11$; supplemental Fig. 3*A*; n-GluA1 cluster intensity: pGSuper, 19.1 ± 1.4 arbitrary units; mut-shRNA, 22.9 ± 0.9 arbitrary units, afadin-shRNA, 20.1 ± 1.5 arbitrary units; $n = 12$; Fig. 3*I*). This suggests that there was no homeostatic compensation, through an increase in GluA1 or GluA2 subunit-containing AMPARs at remaining synapses, in response to the loss of surface-expressed GluA1 and GluA2. Together, these data suggest that afadin is required for the maintenance of synaptic surface expression of GluA1- and GluA2-containing AMPARs.

GluA2-AMPAR Subunit Directly Interacts with Afadin—We next asked how afadin may control the synaptic surface expression of AMPARs. Previously, afadin has been hypothesized to interact directly with GluA2-containing AMPARs via its type II PDZ domain (23, 24), but this has not been confirmed in neurons. In cortical neurons, we found that afadin and GluA2 showed a significant amount of co-localization; 76 ± 3.2% of GluA2 puncta were positive for afadin, whereas, 67.0 ± 3.8% of afadin puncta were positive for GluA2 (Fig. 4*A*). To determine whether afadin forms a protein complex with AMPARs *in vivo*, we performed co-immunoprecipitation experiments from mouse frontal cortex. This revealed that both GluA1 and GluA2 co-immunoprecipitated with both isoforms of afadin, albeit with GluA1 to a lesser extent (Fig. 4*B*). This interaction was confirmed by reciprocal co-immunoprecipitation; L/S-afadin strongly co-immunoprecipitated with GluA2 and to a lesser extent with GluA1 (Fig. 4*C*). To confirm the specificity of these interactions, we co-expressed GFP-tagged GluA1 or GluA2 with myc-L-afadin in HEK293 cells. We found that GFP-GluA2, but not GFP-GluA1, co-immunoprecipitated with myc-L-afadin (Fig. 4*D*), suggesting that afadin principally associated with GluA2 *in situ* and that its interaction with GluA1 may be mediated via its direct interaction with GluA2. It is of note that GluA1 and -2 may be predominantly expressed intracellularly in HEK293 cells. Consistent with this, we have previously shown that afadin is expressed both at the plasma membrane and in the cytosol in HEK293 cells (12), indicating that all proteins are located in similar subcellular locations to test for interactions. Together, these data suggest the interaction of afadin and GluA2 is required for the maintenance of a population of AMPARs at the cell surface and synapses.

DISCUSSION

In this study, we show that knocking down afadin in cortical pyramidal neurons that have already established a complete dendritic field results in reduction of dendritic arborization and the frequency of AMPA receptor-mediated mEPSCs. Furthermore, we demonstrate that loss of afadin is required for the maintenance of a subpopulation of dendritic spines and the surface expression of GluA1 and 2 AMPAR subunits. In addition, we provide evidence that afadin directly interacts with GluA2, potentially via its type II PDZ domain, mechanistically linking the coordination of surface expression of AMPARs to synapse and dendrite structure. Together, these data suggest that afadin is required for the proper maintenance of dendritic fields through the coordinated regulation of both synapse number and function.

In early development, neurite outgrowth is guided by both intrinsic factors, such as transcription factors (5), and extracellular cues, such as neurotrophins (6). Later in development, adhesion proteins and small GTPase signaling help to refine dendritic patterning (2) and establish proper synaptic partners (7, 8). In addition, activity-dependent signals can regulate dendrite arborization but have an opposing effect on synaptic inputs (9). This mechanism, thought to be a homeostatic mechanism, may function to protect developing neurons from over-excitation (9). Recent *in vivo* imaging studies have demonstrated that following the establishment of dendritic fields, these structures remain relatively stable throughout the lifetime of the animal (1, 2). Although extrinsic signals, such as synaptic activity, may induce the bidirectional modeling of dendrites within an established dendritic field, little is known about the molecular mechanisms that are required for the coordinated maintenance of dendritic arborization and excitatory inputs. It has been suggested that molecules required for the establishment of dendritic fields are also involved in their maintenance. Therefore, molecules that coordinately regulate synapse structure and function are good candidates for mediating the stability and maintenance of dendritic fields.

Several classes of proteins, including small GTPases, transcription factors, and adhesion and scaffold proteins, have been shown to affect either dendritic arborization or dendritic spine number but not both parameters (25–31). Indeed, whereas the reduction of dendritic structure would reduce the overall number of synaptic inputs within a dendritic field, these previous studies have indicated that dendrite and synapse structure are not always coordinately regulated. Previous studies have linked afadin with direct interaction with small GTPase proteins, adhesion complexes, and the actin cytoskeleton (11, 12, 15, 19). Moreover, proper afadin signaling has been shown to be required for both Rap- and Rac-dependent remodeling of dendritic spine morphology in mature neurons (15, 19). Furthermore, afadin has been predicted to interact with GluA2-containing AMPARs by a yeast two-hybrid screen (23). These studies support a role for afadin in the maintenance of dendritic arborization and synaptic inputs. Data in the current study build directly on these previous studies and further demonstrate that loss of afadin can coordinately control fields and excitatory inputs of neurons.

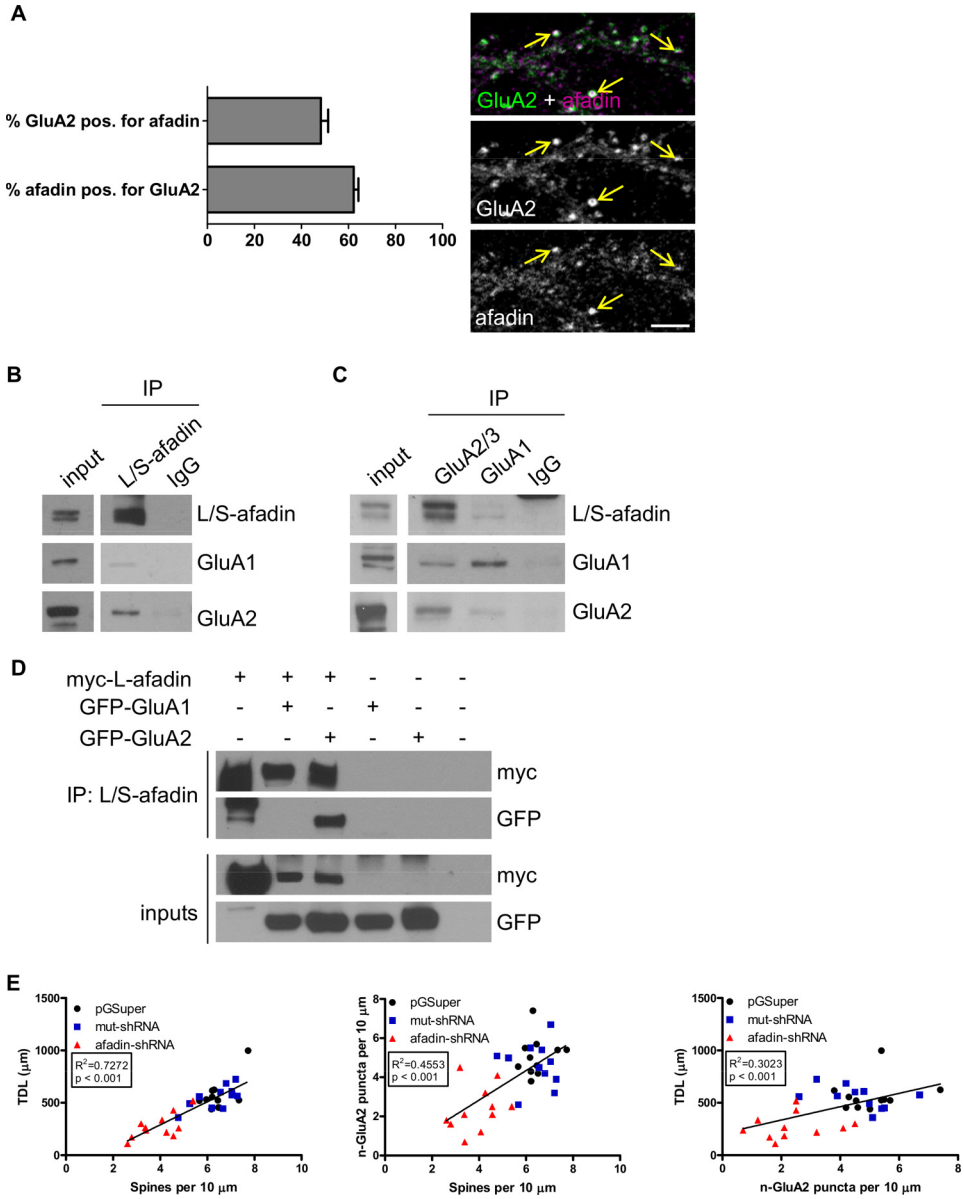

FIGURE 4. **Interaction of afadin with GluA2-containing AMPARs.** *A*, quantification of the percentage of colocalization of afadin and GluA2 in DIV 26 cortical neurons (*right*). *B* and *C*, reciprocal co-immunoprecipitation (*IP*) of afadin with GluA2 and GluA1 from mouse frontal cortex. *D*, co-immunoprecipitation of myc-L-afadin with GFP-GluA2, but not GFP-GluA1, from HEK293 cells. *E*, plots of TDL against spine density or surface GluA2; plot of surface-GluA2 against TDL and spine density in cells expressing pGSuper, control-shRNA, or afadin-shRNA ($n = 11$, r^2 and p values indicated in the *plots*). *Scale bar*, 5 μm. *Error bars*, S.E.

Because measurements of dendrite length, synapse number, and surface expression of GluA2 immunofluorescence parameters were performed in the same cell, we have been able to perform correlation analysis between these parameters. Indeed, TDL showed a strong correlation with TDN, spine density, and surface GluA2; as TDL decreased, TDN, spine density, and surface GluA2 puncta decreased (Fig. 4*E*). Similarly, we found a strong correlation between surface GluA2 puncta and spine density (Fig. 4*E*). A correlation was also observed when comparing TDN with spine density or surface GluA2 (supplemental Fig. 3*B*). These data support a hypothesis that loss of afadin induces a coordinated reduction of dendritic arborization, synapse number, and surface GluA2. It is also interesting to note that similar reductions in both AMPAR-mediated mEPSC frequency and GluA1/2 puncta indicate a reduced number of excitatory synaptic contacts in neurons lacking afadin. The loss of GluA1 could be explained by the loss of GluA1/2 heteromers, induced by the direct interaction of afadin with GluA2. Moreover, the cluster intensities of the remaining GluA2 and GluA1 puncta were equal with both pGSuper and mut-shRNA conditions (Fig. 3, *F* and *I*). Interestingly, an overall reduction in dendritic spine and GluA cluster linear densities could be mediated by the preferential loss of tertiary dendrites as observed in Fig. 2, *A–C*. However, we observed that, whereas spine density was unchanged by afadin knockdown in primary dendrites, spine density was dramatically reduced by afadin knockdown in tertiary dendrites (Fig. 3*C*). Similarly, GluA2 puncta density was reduced in tertiary dendrites (Fig. 3*F*). Thus, the remaining tertiary dendrites in afadin-shRNA-expressing neurons exhibit decreased synapse

density, and the overall effect of reduced synapse densities is not simply mediated by a reduction in tertiary dendrite numbers. These data suggest that, in addition to reducing tertiary dendrite length and number, afadin loss reduces dendritic spine and GluA2 puncta densities on remaining tertiary dendrites and that afadin may be important for coordinating these two morphological features at distal regions in the dendritic arbors of cortical neurons. Together, these data suggest that there was no homeostatic compensation to increase surface GluA2 or GluA1 at remaining synapses, similar to our data from AMPAR-mediated mEPSC amplitude.

Interestingly, a recent study has demonstrated that while afadin is required for the formation of excitatory synapses and normal excitatory transmission in CA1 neurons, there were no observed deficits in dendritic arborization or synaptic expression of AMPARs in these neurons. Although differences in the approach used to investigate the role of afadin in the formation or the maintenance of dendritic fields may account for some of the differences, several other possibilities may exist. Studies in cortical neurons have shown that afadin participates in a pathway required for the remodeling of dendritic spines and the trafficking of AMPARs (12, 15). Moreover, as we demonstrate in the current study, afadin can directly interact with GluA2-containing AMPARs, suggesting that this may provide the link required for the regulation of AMPARs. However, Beaudoin *et al.* (13) did not observe any change in the synaptic expression of AMPARs despite observing reductions in synaptic transmission. As pointed out by the authors of this study, the interactors of afadin may play an important role in determining cell type-specific effects of afadin in hippocampal *versus* cortical neurons. For example, kalirin-7, a direct interactor of afadin and a regulator of AMPAR synaptic expression, is required for the proper formation of dendritic fields in cortical neurons but not for hippocampal neurons (13). As such, it is plausible that the different cellular environment of interacting proteins in cortical and hippocampal neurons may underlie the differences between these two studies. Another possibility is that the role afadin plays during development is different from its role once dendritic fields have been established. In such a scenario, other molecules, such as adhesion or small GTPase signaling proteins, may play an important role in establishing dendritic arborization and the formation of excitatory synapses, whereas afadin takes on a more important role in maintaining dendrite architecture and the number of excitatory inputs.

Several lines of evidence underscore the importance of properly maintained dendritic fields and suggest that active processes underlie the remodeling and maintenance of the dendrites. In neuropsychiatric and neurodevelopmental disorders, such as schizophrenia, intellectual disability, fragile X syndrome, Down syndrome, and autism, dendritic branching and neuronal function are often associated with a concomitant reduction of dendritic arbor complexity and glutamate receptor expression (1, 2, 32, 33). In contrast to deficits observed in disease, sensory stimuli, such as environmental enrichment or sensory deprivation, can result in dendrite outgrowth and rearrangement (34). Thus, elucidating the mechanisms that control maintenance and plasticity of dendrites may have relevance for understanding the pathogenesis of these disorders. Interestingly, afadin is down-regulated in a number of diseases and thus may contribute to the pathophysiology in these disorders, but the cellular consequences of down-regulating afadin are not clear. The chromosomal region containing the afadin gene (6q27) has been associated with biopolar disorder, intellectual disability, and Alzheimer disease (17, 24, 35, 36), suggesting a possible role of genes in this region in the pathophysiology of these disorders. Furthermore, afadin expression is reportedly reduced in the brains of schizophrenic patients (37). Taken together, our findings indicate that afadin is required for the coordinated maintenance of both the dendritic field and synaptic AMPARs in pyramidal neurons. Such coordinated mechanisms are thought to contribute to the maintenance of neural circuits within the brain (1, 2) and might contribute to the simultaneous impairments in neuronal structure and function reported in several neuropsychiatric disorders.

REFERENCES

1. Jan, Y. N., and Jan, L. Y. (2010) Branching out. Mechanisms of dendritic arborization. *Nat. Rev. Neurosci.* **11,** 316–328
2. Parrish, J. Z., Emoto, K., Kim, M. D., and Jan, Y. N. (2007) Mechanisms that regulate establishment, maintenance, and remodeling of dendritic fields. *Annu. Rev. Neurosci.* **30,** 399–423
3. London, M., and Häusser, M. (2005) Dendritic computation. *Annu. Rev. Neurosci.* **28,** 503–532
4. Spruston, N. (2008) Pyramidal neurons. Dendritic structure and synaptic integration. *Nat. Rev. Neurosci.* **9,** 206–221
5. Parrish, J. Z., Kim, M. D., Jan, L. Y., and Jan, Y. N. (2006) Genome-wide analyses identify transcription factors required for proper morphogenesis of *Drosophila* sensory neuron dendrites. *Genes Dev.* **20,** 820–835
6. McAllister, A. K., Katz, L. C., and Lo, D. C. (1997) Opposing roles for endogenous BDNF and NT-3 in regulating cortical dendritic growth. *Neuron* **18,** 767–778
7. Yamagata, M., Weiner, J. A., and Sanes, J. R. (2002) Sidekicks. Synaptic adhesion molecules that promote lamina-specific connectivity in the retina. *Cell* **110,** 649–660
8. Togashi, H., Miyoshi, J., Honda, T., Sakisaka, T., Takai, Y., and Takeichi, M. (2006) Interneurite affinity is regulated by heterophilic nectin interactions in concert with the cadherin machinery. *J. Cell Biol.* **174,** 141–151
9. Peng, Y. R., He, S., Marie, H., Zeng, S. Y., Ma, J., Tan, Z. J., Lee, S. Y., Malenka, R. C., and Yu, X. (2009) Coordinated changes in dendritic arborization and synaptic strength during neural circuit development. *Neuron* **61,** 71–84
10. Yu, X., and Malenka, R. C. (2003) β-Catenin is critical for dendritic morphogenesis. *Nat. Neurosci.* **6,** 1169–1177
11. Takai, Y., Ikeda, W., Ogita, H., and Rikitake, Y. (2008) The immunoglobulin-like cell adhesion molecule nectin and its associated protein afadin. *Annu. Rev. Cell Dev. Biol.* **24,** 309–342
12. Xie, Z., Photowala, H., Cahill, M. E., Srivastava, D. P., Woolfrey, K. M., Shum, C. Y., Huganir, R. L., and Penzes, P. (2008) Coordination of synaptic adhesion with dendritic spine remodeling by AF-6 and kalirin-7. *J. Neurosci.* **28,** 6079–6091
13. Beaudoin, G. M., 3rd, Schofield, C. M., Nuwal, T., Zang, K., Ullian, E. M., Huang, B., and Reichardt, L. F. (2012) Afadin, a Ras/Rap effector that controls cadherin function, promotes spine and excitatory synapse density in the hippocampus. *J. Neurosci.* **32,** 99–110
14. Majima, T., Ogita, H., Yamada, T., Amano, H., Togashi, H., Sakisaka, T., Tanaka-Okamoto, M., Ishizaki, H., Miyoshi, J., and Takai, Y. (2009) Involvement of afadin in the formation and remodeling of synapses in the hippocampus. *Biochem. Biophys. Res. Commun.* **385,** 539–544
15. Xie, Z., Huganir, R. L., and Penzes, P. (2005) Activity-dependent dendritic spine structural plasticity is regulated by small GTPase Rap1 and its target AF-6. *Neuron* **48,** 605–618
16. Srivastava, D. P., Woolfrey, K. M., and Penzes, P. (2011) Analysis of dendritic spine morphology in cultured CNS neurons. *J. Vis. Exp.* **13,** e2794

17. Srivastava, D. P., Woolfrey, K. M., Jones, K. A., Anderson, C. T., Smith, K. R., Russell, T. A., Lee, H., Yasvoina, M. V., Wokosin, D. L., Ozdinler, P. H., Shepherd, G. M., and Penzes, P. (2012) An autism-associated variant of Epac2 reveals a role for Ras/Epac2 signaling in controlling basal dendrite maintenance in mice. *PLoS Biol.* **10,** e1001350
18. Kojima, S., Vignjevic, D., and Borisy, G. G. (2004) Improved silencing vector co-expressing GFP and small hairpin RNA. *BioTechniques* **36,** 74–79
19. Srivastava, D. P., Woolfrey, K. M., Jones, K. A., Shum, C. Y., Lash, L. L., Swanson, G. T., and Penzes, P. (2008) Rapid enhancement of two-step wiring plasticity by estrogen and NMDA receptor activity. *Proc. Natl. Acad. Sci. U.S.A.* **105,** 14650–14655
20. Woolfrey, K. M., Srivastava, D. P., Photowala, H., Yamashita, M., Barbolina, M. V., Cahill, M. E., Xie, Z., Jones, K. A., Quilliam, L. A., Prakriya, M., and Penzes, P. (2009) Epac2 induces synapse remodeling and depression and its disease-associated forms alter spines. *Nat. Neurosci.* **12,** 1275–1284
21. Buchert, M., Schneider, S., Meskenaite, V., Adams, M. T., Canaani, E., Baechi, T., Moelling, K., and Hovens, C. M. (1999) The junction-associated protein AF-6 interacts and clusters with specific Eph receptor tyrosine kinases at specialized sites of cell-cell contact in the brain. *J. Cell Biol.* **144,** 361–371
22. Nishioka, H., Mizoguchi, A., Nakanishi, H., Mandai, K., Takahashi, K., Kimura, K., Satoh-Moriya, A., and Takai, Y. (2000) Localization of L-afadin at puncta adhaerentia-like junctions between the mossy fiber terminals and the dendritic trunks of pyramidal cells in the adult mouse hippocampus. *J. Comp. Neurol.* **424,** 297–306
23. Malinow, R., and Malenka, R. C. (2002) AMPA receptor trafficking and synaptic plasticity. *Annu. Rev. Neurosci.* **25,** 103–126
24. Rogers, C. A., Maron, C., Schulteis, C., Allen, W. R., and Heinemann, S. F. (2001) Afadin, a link between AMPA receptors and the actin cytoskeleton. *Soc. Neurosci. Abstr.* **27,** 32.16
25. Arikkath, J. (2009) Regulation of dendrite and spine morphogenesis and plasticity by catenins. *Mol. Neurobiol.* **40,** 46–54
26. Charych, E. I., Akum, B. F., Goldberg, J. S., Jörnsten, R. J., Rongo, C., Zheng, J. Q., and Firestein, B. L. (2006) Activity-independent regulation of dendrite patterning by postsynaptic density protein PSD-95. *J. Neurosci.* **26,** 10164–10176
27. Chow, D. K., Groszer, M., Pribadi, M., Machniki, M., Carmichael, S. T., Liu, X., and Trachtenberg, J. T. (2009) Laminar and compartmental regulation of dendritic growth in mature cortex. *Nat. Neurosci.* **12,** 116–118
28. El-Husseini, A. E., Schnell, E., Chetkovich, D. M., Nicoll, R. A., and Bredt, D. S. (2000) PSD-95 involvement in maturation of excitatory synapses. *Science* **290,** 1364–1368
29. Huang, W., Zhou, Z., Asrar, S., Henkelman, M., Xie, W., and Jia, Z. (2011) p21-activated kinases 1 and 3 control brain size through coordinating neuronal complexity and synaptic properties. *Mol. Cell Biol.* **31,** 388–403
30. Lin, Y. C., and Koleske, A. J. (2010) Mechanisms of synapse and dendrite maintenance and their disruption in psychiatric and neurodegenerative disorders. *Annu. Rev. Neurosci.* **33,** 349–378
31. Zhou, Z., Hong, E. J., Cohen, S., Zhao, W. N., Ho, H. Y., Schmidt, L., Chen, W. G., Lin, Y., Savner, E., Griffith, E. C., Hu, L., Steen, J. A., Weitz, C. J., and Greenberg, M. E. (2006) Brain-specific phosphorylation of MeCP2 regulates activity-dependent Bdnf transcription, dendritic growth, and spine maturation. *Neuron* **52,** 255–269
32. Kaufmann, W. E., and Moser, H. W. (2000) Dendritic anomalies in disorders associated with mental retardation. *Cereb. Cortex* **10,** 981–991
33. Raymond, G. V., Bauman, M. L., and Kemper, T. L. (1996) Hippocampus in autism. A Golgi analysis. *Acta Neuropathol.* **91,** 117–119
34. Greenough, W. (1984) Structural correlates of information storage in mammalian brain. A review and hypothesis. *Trends Neurosci.* **7,** 229–233
35. Weiss, L. A., Arking, D. E., Gene Discovery Project of Johns Hopkins & the Autism Consortium, Daly, M. J., and Chakravarti, A. (2009) A genome-wide linkage and association scan reveals novel loci for autism. *Nature* **461,** 802–808
36. Yang, S., Wang, K., Gregory, B., Berrettini, W., Wang, L. S., Hakonarson, H., and Bucan, M. (2009) Genomic landscape of a three-generation pedigree segregating affective disorder. *PLoS One* **4,** e4474
37. Katsel, P., Davis, K. L., and Haroutunian, V. (2005) Variations in myelin and oligodendrocyte-related gene expression across multiple brain regions in schizophrenia. A gene ontology study. *Schizophr. Res.* **79,** 157–173